Formation of aroma-potent thiols in heat-stable vegetable oil-in-water emulsion models containing ribose and cysteine

Food Research International 231 (2026) 118600

Contents lists available at ScienceDirect

Food Research International

journal homepage: www.elsevier.com/locate/foodres

Formation of aroma-potent thiols in heat-stable vegetable oil-in-water emulsion models containing ribose and cysteine

Suleyman Yiltirak [a], Dimitris P. Balagiannis [a], Jan Koek [b], Jens Koch [c], J. Stephen Elmore [a,*]

[a] Department of Food and Nutritional Sciences, University of Reading, Whiteknights, Reading RG6 6DZ, UK
[b] Foods Innovation Centre Unilever, Bronland 14, 6708, WH, Wageningen, the Netherlands
[c] Symrise AG, Mühlenfeldstraße 1, 37603 Holzminden, Germany

ARTICLE INFO

Keywords:
Meaty thiols
2-methyl-3-furanthiol
2-furfurylthiol
Emulsion stability
Particle size distribution

ABSTRACT

To improve the aroma profile of meat alternatives, savory process flavorings are often incorporated into the plant-based matrix as top notes to enhance meaty character. However, aroma addition remains a significant cost factor, and achieving an authentic meat aroma profile is still difficult, resulting in consumer dissatisfaction. The marble-like structure in raw meat creates an emulsion interface and it might have a key role in enhancing desirable meat aroma. This study investigated the formation of 2-furfurylthiol (FFT), 2-methyl-3-furanthiol (MFT), and 3-mercapto-2-butanone (3M2B) as important contributors to the aroma of cooked meat in emulsion models. Firstly, the characterizations of emulsion and emulsifiers were evaluated before and after heating. Sucrose ester PS750 at 3% was found to be the best-performing emulsifier for developing heat-stable emulsions. Emulsions containing ribose and cysteine in aqueous buffer, canola oil (10%), and sucrose ester (3%) were prepared by high-pressure homogenization, and then heated at 100 °C, 110 °C, 120 °C and 130 °C for 4 h, 2 h, 1 h, and 0.5 h, respectively. In general, the highest concentrations of meaty thiols were observed after heating at 100 °C for 4 h, while higher temperatures with shorter heating times decreased their levels. A key finding was that the amount of MFT and FFT in emulsions almost doubled at 100 °C and 110 °C relative to the control (the same ingredients but without emulsifier). This work provides valuable insights into cost-effective strategies for enriching the meaty aroma of plant-based meat analogs.

1. Introduction

Consumption of meat and meat products has become a frequently discussed issue in recent years due to ethical concerns regarding environmental damage, animal rights, and health problems linked to heart disease (van der Sluis et al., 2026). However, plant-based meat analogs/replacers suffer from lack of meaty aroma production upon heating. Hence, meaty aromas need to be incorporated at relatively high levels (3–10%), which significantly increases raw material costs (Ahmad et al., 2022). In order to be cost-attractive for consumers, the products should be at least equal in price and preferably less expensive than the meat equivalent (Warner, 2024). The industry seeks more cost-effective aroma with a closer profile to the real meat experience, as, currently, the aroma of cooked meat analogs fails to meet consumers' sensory expectations (Appiani et al., 2023).

Characteristic meat aroma is derived from thermal processing where Maillard reaction, lipid oxidation, and vitamin degradation occur (Parker, 2017). The key precursors of a generic meaty aroma are cysteine and reducing sugars, especially the pentose sugars ribose and xylose (Parker, 2017). During heating, these precursors undergo a series of multi-step reactions resulting in numerous classes of volatile compounds *via* the Maillard reaction (Bleicher et al., 2022; Zamora & Hidalgo, 2005). Despite the variety of volatiles produced, only a small proportion contributes significantly to aroma development (Dunkel et al., 2014). Three compounds formed in cysteine/pentose model systems during heating, namely 2-methyl-3-furanthiol (MFT), 2-furfurylthiol (FFT), and 3-mercapto-2-butanone (3M2B), are all highly important for overall meaty aroma profile (Cerny, 2012; Cerny & Davidek, 2003). The odor thresholds of MFT and FFT are similar and have been reported as low as 0.0025–0.01 ng/L in air, while the 3M2B odor threshold ranges between 0.2 and 0.8 ng/L in air, highlighting their key roles in cooked meat aroma (Hofmann & Schieberle, 1995).

Micelles in emulsion systems can create unique regions at droplet interfaces due to their amphiphilic nature. Early studies on the

* Corresponding author.
E-mail address: j.s.elmore@reading.ac.uk (J.S. Elmore).

https://doi.org/10.1016/j.foodres.2026.118600
Received 2 October 2025; Received in revised form 29 January 2026; Accepted 2 February 2026
Available online 3 February 2026

microemulsion interface examined the potent aroma compounds in meaty mixtures, especially FFT (Vauthey et al., 2000; Yaghmur et al., 2002, 2005) and MFT (Vauthey et al., 2000), and their formation mechanisms. These studies proposed that the reactant accumulation at the interface could increase reaction rates (micro-emulsion catalysis) and also could lead to new aroma formation pathways (Sagalowicz et al., 2006; Yaghmur et al., 2002, 2005). Binary self-assembly micro-emulsions (Blank et al., 2006; Sagalowicz et al., 2016; Vauthey et al., 2000) and multicomponent/U-type microemulsions (Fanun et al., 2001; Lutz & Garti, 2005; Yaghmur et al., 2002, 2005) may induce the Maillard reaction due to their very small particle sizes. Recent studies focused on homogenization techniques to create smaller emulsion droplets by high pressure before heating, which promoted the formation of early glycation products (Troise et al., 2016; Troise, Fogliano, et al., 2020), Strecker aldehydes (Troise, Fogliano, et al., 2020), and taste-active molecules (Troise, Berton-Carabin, et al., 2020) using vegetable oil or medium chain triglycerides during heating.

Emulsion stability is often described as resistance to physical changes over time and during processing (McClements & Jafari, 2018). One of the important parameters is particle size, since phase separation is strongly correlated with larger droplet counts *via* flocculation, coalescence, and gravitational separation (McClements & Jafari, 2018). The nature of the emulsifier and its ratio to oil affect the kinetic stability of emulsions, where an energy barrier created by mechanical force allows the emulsion to stay in one phase (McClements & Gumus, 2016; Rao & McClements, 2011). In most cases, an emulsifier is expected to have a fast absorption ability at the oil-water interface and reduce the interfacial tension, thus preventing droplet aggregation. Additionally, the emulsifier should have heat resistance to maintain its physical condition during cooking or pasteurization and also to support Maillard-type aroma generation.

In this study, different emulsion systems were prepared and heated to investigate the formation of key aroma compounds, including MFT, FFT, and 3M2B. These emulsions might offer insights into preparation methods to obtain more intense flavors, thereby allowing for lower and more cost-effective formulation levels when applied to vegetable oil-based products. Previous studies primarily used monoglyceride-based microemulsion models, where monoglycerides serve as both lipid and surfactant, or multicomponent microemulsions based on R-(+)-limonene – a compound with a strong citrus flavor – to generate meaty aroma. However, such systems are thermally sensitive and prone to structural changes with changing temperature and component ratios.

The aim of this study was to analyze emulsion-based systems designed to enhance meaty aroma and enable their potential incorporation into plant-based products lacking meaty aroma. This study used canola oil as an oil phase and sucrose ester as a plant-based emulsifier. Emulsions were prepared using a homogenizer to produce nano-scale particles, which made them more applicable to food systems while avoiding excessive usage of surfactants/cosurfactants. Accordingly, the model systems, comprising only food-grade ingredients, were designed as: (i) emulsion containing buffer/oil/emulsifier, (ii) buffer/canola oil (without emulsifier), (iii) buffer/emulsifier, and (iv) buffer alone, all containing cysteine and ribose. Samples were subjected to multiple thermal treatments at 100 °C for 4 h, 110 °C for 2 h, 120 °C for 1 h, and 130 °C for 0.5 h. Emulsion stability and emulsifiers were tested during heating, ensuring the one-phase structure and heat stability of emulsion particles.

2. Methods and materials

2.1. Chemicals and consumables

L-Cysteine (≥97%), D-(−)-ribose (≥98%), 2-methyl-3-furanthiol (99%), 2,3,4,5,6-pentafluorobenzyl bromide (99%) and Tween 20 (polyoxyethylene (20) sorbitan monolaurate – HLB 16.7) were supplied by Sigma-Aldrich Co. (Gillingham, UK). 2-Furfurylthiol (99%) and 3-mercapto-2-butanone (99%) were purchased from Tokyo Chemical Industry UK Ltd. (Oxford, UK). 2-(Methyl-d_3)-3-furanthiol (MFT-d3) and 2-furfuryl-α,α-d_2-thiol (FFT-d3) were obtained from aromaLAB GmbH (Martinsried, Germany). L-(+)-Tartaric acid (99%) and sodium hydroxide (white pellets, >97%) were purchased from Fisher Scientific (Loughborough, UK). Potassium dihydrogen phosphate (99%) and dipotassium hydrogen phosphate (98%; food grade) were purchased from APC Pure (Hyde, UK). Sucrose esters (PS750 (HLB 16) and SP50 (HLB 11); food grade) were supplied by Sisterna (Roosendaal, The Netherlands). Finally, canola oil (rapeseed vegetable oil: supermarket own brand) was purchased from a local supermarket.

According to manufacturer's specifications, PS750 and SP50 contain 75% monoesters and 50% monoesters, respectively. These sucrose esters were produced by esterification of sucrose from sugar cane with palmitate/stearate from palm oil.

Potassium phosphate buffer (0.5 M, pH 5.5) was made using potassium dihydrogen phosphate and dipotassium hydrogen phosphate in tap water.

2.2. Emulsion preparation and selection of emulsion composition for heating

Emulsification was achieved in three steps (Kampa, Frazier, & Rodriguez-Garcia, 2022). Firstly, sucrose ester and potassium phosphate buffer (0.5 M, pH 5.5) (aqueous phase) were mixed with a magnetic stirrer for 30 min at 30 °C. Subsequently, canola oil was added and mixed for a further 5 min. In the second step, a coarse emulsion was obtained by using a high-shear mixer (Silverson Machines Ltd., Chesham, UK) for 10 min at 7000 rpm. The last step was completed by passing 600 mL of coarse emulsion through a Panda high-pressure homogenizer (GEA Group, Düsseldorf, Germany) at 300 bar with a single cycle.

To select a suitable emulsifier for further experiments, the particle size distribution of emulsions prepared with Tween 20 and two different sucrose esters (namely PS750 and SP50) were studied before and after heating at 100 °C for 4 h. These non-ionic emulsifiers have different structures (polysorbate and ester) and hydrophilic-lipophilic balance (HLB) values. They were prepared in three steps, as explained above. The particle size stability of emulsions was monitored before and during heating at 100 °C for 4 h. The canola oil content (*w/w*) of the emulsion was set to 10%. After the selection of sucrose ester PS750 as an emulsifier, different concentrations from 2% to 4% (*w/w*) were compared with regards to their particle size distribution during heating at 100 °C for 4 h and 130 °C for 0.5 h. This piece of work aimed to minimize the contribution of emulsifier to the formation of volatile compounds by reducing the emulsifier content in emulsion models. Additionally, the canola oil content (10%, *w/w*) was selected as representing a similar fat content to that of lean beef meat (André et al., 2025). Canola oil was chosen as a widely used household vegetable oil with a high oleic acid content (up to 65%) and a low saturated fatty acid composition (<7%) (Ghazani et al., 2016). According to the manufacturer's declaration, canola oil contains 7.3 g of total saturated fatty acids, 58 g of total monounsaturated fatty acids, and 27 g of total polyunsaturated fatty acids per 100 mL of oil. The aim was to limit the polyunsaturated fatty acid content in the vegetable oil to reduce the formation of excessive lipid oxidation products while avoiding the characteristic aroma notes associated with the vegetable source. All emulsions were prepared and analyzed in triplicate.

2.3. Preparation of reaction model systems

After the determination of particle size distributions in emulsions, a sucrose ester concentration (PS750) of 3% for the emulsion system was chosen for subsequent studies. Four different models were prepared to understand the effect of interface with and without oil on the formation of potent thiol compounds. The models were: i) emulsion system (87%

buffer, 3% sucrose ester, 10% canola oil), ii) buffer/oil system (90% buffer, 10% canola oil), iii) buffer/emulsifier (97% buffer, 3% sucrose ester), iv) buffer system (100% buffer). All buffer phases were prepared by dissolving ribose (25 mM) and cysteine (25 mM) in potassium phosphate buffer (0.5 M, pH 5.5). The emulsification procedure was applied to all systems.

2.4. Heating of samples

After emulsification, model systems (3 mL) with 3% sucrose ester (PS750) were transferred to 20-mL Duran tubes with screw-caps lined with PTFE gaskets (Duran Wheaton Kimble, Werthein, Germany) and they were heated at 100 °C/4 h, 110 °C/2 h, 120 °C/1 h and 130 °C/0.5 h in a heating block equipped with a magnetic stirrer (RS900 reaction station; Electrochemical, Cambridge, UK). These temperature combinations were selected as practical experimental conditions to represent slow and fast cooking techniques for creating meat aroma (Miao et al., 2024). PTFE-covered magnetic stir bars (12 mm × 4.5 mm) were used during heating to help maintain the one-phase emulsion structure. After heating, the tubes were cooled immediately to room temperature in an ice bath to stop the thermal reaction. Subsequently, they were flushed with Pureshield Argon (B.O.C., UK) to prevent further oxidation and stored at −20 °C until analysis. Each heating condition was conducted three times. All systems without precursors were prepared and heated under the same conditions and used as blanks for aroma analysis.

2.5. Derivatization of thiol-containing aroma compounds

Thiol compounds in heated samples were derivatized, as reported previously (Capone et al., 2011), with some modifications. An aliquot of sample (30 µL) was mixed and vortexed with 10 µL of 20 µg/L MFT-d3 and FFT-d2, and extracted with 6 mL ice-cold NaOH (1 M) in a 20-mL vial with metal screw-cap and septum, suitable for solid-phase microextraction (SPME). Then, derivatization was performed by adding 50 µL of pentafluorobenzyl bromide (PFBBr) solution (20 µL of PFBBr in 50 mL redistilled ethanol), vortex mixing and resting at room temperature for 10–15 min to allow the reaction to proceed. Tartaric acid (0.5 g) was added to reduce the pH to between 4 and 5, to stop the derivatization reaction as well as to optimize SPME extraction and MS detection (Capone et al., 2011).

2.6. Analysis of thiol-containing aroma compounds by solid-phase microextraction (SPME)-gas chromatography-mass spectrometry (GC-MS)

A 20-mL SPME vial containing the derivatized thiol compounds was placed in an Agilent 110 headspace autosampler coupled to an Agilent 7890A gas chromatography (GC) system (Agilent Technologies, Santa Clara, CA) attached to a 5975C inert MSD triple-axis detector. A 50/30 µm divinylbenzene/Carboxen™ on poly(dimethylsiloxane) SPME fiber (Supelco, Bellefonte, PA) was used for extraction of derivatized thiol volatiles. After equilibration (80 °C/30 min), the SPME fiber was exposed to the sample headspace at 80 °C for 20 min and then desorbed into the injection port for 20 min in splitless mode at 250 °C, the splitter opening after 45 s. The injection port liner was appropriate for SPME analysis (Merck – Part No. 2637505). The chromatographic separation was carried out with a DB-5MS capillary column (30 m × 0.25 mm × 1 µm film thickness; Agilent, Santa Clara, CA). Helium was used as the carrier gas at a constant flow rate of 1.2 mL/min. The temperature program used was 2 min at 40 °C with an increase of 4 °C/min to 280 °C. Mass spectra in electron impact mode (EI) were measured at 70 eV and selected ion monitoring (SIM) was used for quantification. The ions recorded were *m/z* 113, 181, 296 for MFT, *m/z* 116, 181, 297 for MFT-d3, *m/z* 81, 181, 294 for FFT, *m/z* 83, 181, 296 for FFT-d2 and *m/z* 72, 241, 181, 284 for 3M2B (Fig. S1 and S2). Analysis was performed in triplicate for each sample. Concentrations were determined by using a matrix-matched calibration curve prepared from an unheated emulsion containing equal amounts of internal standards as the samples, where the concentration of the spiked MFT and FFT ranged from 0.2 µg/L to 10 µg/L. Limit of detection (LOD) and limit of quantification (LOQ) were calculated based on the standard deviation of a linear response and a slope (Fig. S3 and Table S1) (International Council for Harmonisation, 2023).

2.7. Physicochemical characterization of emulsion

2.7.1. Particle size analysis

Particle size ($d_{3,2}$ and $d_{4,3}$), particle size distribution, and span value of unheated and heated emulsions were obtained at room temperature by using static light scattering (Mastersizer 2000; Malvern Instruments, Malvern, UK), as reported previously (Giles et al., 2025) with some modifications. The instrument was equipped with a liquid dispersing unit with a stirring cell and a 300F lens. Samples were added to the cell unit using a plastic pipette. The proportion of light scattered by the particles, obscuration, was adjusted to between 13% and 15%. Background noise and contamination were corrected before analysis. The cell was rinsed with hot tap water three times after each measurement. All measurements were repeated three times. The data were collected using Malvern software, Mastersizer-S v2.19.

2.7.2. Viscosity analysis

Viscosity analysis was carried out by modular compact rheometer (MCR 302; Anton Paar, St. Albans, UK) in the unheated and heated emulsions prepared with Tween 20 and PS750, before and after heating at 100 °C for 4 h, as previously reported (Giles et al., 2025), with some modifications. The instrument was coupled with a smooth rotating concentric cylinder and measuring cup (CC27 system). An aliquot (20 mL) of sample was transferred into the measuring cup (gap size 1 mm) and allowed to equilibrate for 300 s at 20 °C prior to measurements. Viscosity measurements were over a shear rate range of 0.1–1000 s^{-1} using 15 measurement steps. All measurements were performed in duplicate for each sample.

2.7.3. Creaming index

Creaming index was determined according to the method described previously (Kampa, Frazier et al., 2022). Emulsions prepared with PS750, and Tween 20 were used to observe the effect of different emulsifiers on emulsion stability before and after heating. at 100 °C for 4 h. Aliquots (3 mL) of unheated and heated emulsion samples were stored at 4 °C, 20 °C and 40 °C. The total height (mm) and top layer (mm) were recorded with a digital caliper after 2, 3, 7, 10 and 20 days. Creaming index (%) was calculated using the equation:

$$\textit{Creaming Index}\ (\%) = \left(\frac{\textit{Top Layer}}{\textit{Total Height}} \right) \times 100$$

All measurements were taken in duplicate for each sample.

2.7.4. Surface tension and interfacial tension analysis

The surface tension, interfacial tension, and critical micelle concentration (CMC) were evaluated according to the method described previously (Kampa, Koidis, et al., 2022), with some modifications. The surface tension measurements of deionized water–air and canola oil–air were conducted using a pendant drop analyzer (DS4270; Krüss GmbH, Hamburg, Germany) at 20 °C. A suspended drop (5 µL) of water or canola oil from a needle (0.9 mm outer diameter) in air was allowed to stabilize for 30 min until reaching the characteristic pear-shape equilibrium.

Interfacial tension between water and canola oil was measured by forming a suspended water droplet (5 µL) at the needle tip inside a quartz cuvette containing canola oil under the same experimental conditions. Interfacial tension between emulsifier solutions (Tween 20 at

3% (*w/w*) or PS750 at 3% (*w/w*)) prepared in deionized water and canola oil was determined using the same pendant drop configuration.

The critical micelle concentration (CMC) of Tween 20 and PS750 was determined from surface tension measurements of emulsifier solutions in air using the pendant drop method. A series of emulsifier concentrations (0, 0.0001, 0.0005, 0.0007, 0.001, 0.002, 0.005, 0.01, 0.05, 0.1, and 0.5% (*w/w*)) were prepared in deionized water, and the surface tension was measured at 20 °C. The CMC was identified as the breakpoint in the plot of surface tension *versus* emulsifier concentration. All measurements were conducted in triplicate.

2.8. Statistical analysis

The results were reported as mean ± standard deviation. One-way ANOVA was performed with Tukey test (XLSTAT Sensory, version 2022.5.1.1388; Lumivero, Denver, CO) to observe statistical differences ($p < 0.05$).

3. Results and discussion

3.1. Selection of emulsifier

Three different emulsifiers (Tween 20, and the sucrose esters PS750 and SP50) were tested on their ability to form a suitable emulsion before and after heating at 100 °C for 4 h. These model emulsions were a mixture of buffer (87%), canola oil (10%), and corresponding emulsifier (3%). After homogenization/before heating, it was observed that Tween 20 had a lower span value compared to SP50 and PS750, meaning that Tween 20 showed better particle size uniformity (Table 1). After homogenization, due to its rapid adsorption ability in the emulsion, Tween 20 showed a sharper distribution with lower large volume fractions (especially between 10 μm and 1000 μm) compared to emulsions with sucrose esters, as smaller emulsifiers can act much more quickly than bigger emulsifiers, preventing further droplet break-up under pressure (McClements & Jafari, 2018). However, the span value for Tween 20 increased from 2.79 ± 0.04 to 5.27 ± 1.14 after heating at 100 °C for 4 h. As seen in Fig. 1, the heated emulsion with Tween 20 separated into two phases; in particular, particle sizes between 50 and 100 μm were present at a higher volume fraction (up to 12.1%) compared to SP50 and PS750, after heating at 100 °C for 4 h (Table 1). On the other hand, these larger particle sizes for SP50 and PS750 decreased or disappeared upon heating, respectively. As Tween 20 has a cloud point of 76 °C, it starts to aggregate above this temperature, becoming more turbid and increasing in particle size (McClements, 2004).

Among the two sucrose esters with different HLB values, PS750 (HLB 16) showed better stability than SP50 (HLB 11), both before and after heating at 100 °C for 4 h (Table 1). Despite the observation that heating reduced the larger particle sizes between 50 μm and 1000 μm (Table 1) in both emulsions prepared with SP50 and PS750, the span value of PS750 was lower than SP50, mainly because the percentage volume of SP50 between 50 and 1000 μm was higher. Therefore, PS750 was selected for further emulsion preparation, as it showed better particle size distribution before and after heating.

3.2. Physicochemical characterization of emulsions

3.2.1. Particle size and distribution of emulsion models with variable emulsifier content

The particle size distributions of emulsions prepared with 2%, 3%, and 4% sucrose ester (PS750) and 10% canola oil during heating over 5 h at 100 °C are shown in Fig. 2A. Emulsions were relatively stable for the first 3 h and exhibited a wider distribution, especially after 5 h of heating, compared to unheated emulsions. The mean droplet diameter based on area ($d_{3,2}$) ranged from 0.25 to 0.31 μm in all emulsions, both before and after heating. The volume fractions for larger particles (1–10 μm and 10–50 μm), especially at higher sucrose ester concentrations (4%), tended to increase after prolonged heating, as excessive emulsifier concentrations formed emulsifier micelles without oil (McClements & Jafari, 2018). Emulsions experienced a breaking point, where they started to show a second shoulder, after 4 h or 5 h of heating, compared to unheated ones, which can be seen from volume fractions between 10 μm and 100 μm in Table 2 and Fig. 2.

In emulsions, the particle size volume fraction between 0.1 and 1 μm (diameter) generally decreased after 3 h of heating but increased after 4 and 5 h of heating, along with the mean droplet diameter based on volume ($d_{4,3}$) (Table 2). On the other hand, the fraction 1–10 μm in emulsions with 2% and 3% emulsifier increased after 3 h, then started to shift to bigger size fractions after heating for 4 h, compared to unheated emulsions. Conceivably, the sucrose ester and canola oil solubility increased under mild heating conditions (Rao & McClements, 2011), and emulsion droplets started to aggregate under extended heat treatment.

Similarly, the span value tended to increase with heating time, indicating that the particle size distribution became less uniform as heating continued. Span value increased by 27%, 18%, and 102% in emulsions with 2%, 3%, and 4% sucrose ester, respectively, after 4 h of heating, compared to unheated emulsions. For the context of this study, the emulsion with the lowest span value after 4 h heating was accepted as the most stable emulsion. Consequently, the emulsion system containing precursors resulted in a similar trend of span value to the emulsion without precursors, remaining stable up to 4 h and then reaching 3.92 ± 0.05 after heating for 5 h at 100 °C (Table 2). The mean droplet diameter ($d_{3,2}$) was between 0.24 and 0.28 μm in emulsions with precursors (Table 2). It was possible that the Maillard reaction allowed the emulsion to have more resistance against heat treatment at 100 °C for 4 h due to the formation of advanced Maillard reaction products, helping the emulsion structure at the interface (Feng et al., 2022), compared to the emulsion (3%) without precursors. At 130 °C, the percentage volume fraction of larger particle fractions (10–50 μm) reached a maximum after 45 min. Increasing the heating temperature resulted in faster formation of larger droplets in emulsions.

3.2.2. Creaming of emulsions

The creaming index (%) of unheated and heated emulsions prepared with Tween 20 (3%) and PS750 (2%, 3%, and 4%) was monitored over 20 days at 4 °C, 20 °C, and 40 °C to evaluate the effects of storage temperature and emulsifier type on emulsion stability after heating. Emulsions prepared with PS750 remained stable at 4 °C and 20 °C, with

Table 1
Comparison of physical characteristics of emulsions prepared using Tween 20, SP50 and PS750 before (0 h) and after heating (4 h).*

					% Volume fraction				
Temperature	**Time**	**Span value**	**$D_{3,2}$ (μm)**	**$D_{4,3}$ (μm)**	**0.1–1 μm**	**1–10 μm**	**10–50 μm**	**50–100 μm**	**100–1000 μm**
Tween 20	0 h	2.79 ± 0.04^{c}	0.38 ± 0.07^{b}	0.88 ± 0.06^{b}	68.74 ± 0.41^{c}	31.26 ± 0.19^{a}	0.00	0.00	0.00
	4 h	5.27 ± 1.14^{a}	1.36 ± 0.27^{a}	85.65 ± 12.75^{a}	29.43 ± 0.18^{d}	14.45 ± 0.08^{d}	7.85 ± 0.07^{a}	12.13 ± 0.07^{a}	0.00
SP50	0 h	5.38 ± 0.54^{a}	0.25 ± 0.02^{b}	1.84 ± 0.21^{b}	82.77 ± 0.49^{ab}	14.19 ± 0.09^{d}	2.56 ± 0.02^{c}	0.25 ± 0.02^{b}	0.26 ± 0.01^{a}
	4 h	4.71 ± 0.43^{ab}	0.30 ± 0.04^{b}	1.36 ± 0.06^{b}	80.45 ± 0.48^{b}	17.77 ± 0.11^{b}	1.54 ± 0.01^{d}	0.06 ± 0.01^{cd}	0.16 ± 0.01^{b}
PS750	0 h	3.23 ± 0.03^{c}	0.26 ± 0.01^{b}	0.81 ± 0.09^{b}	83.83 ± 0.51^{a}	15.37 ± 0.09^{c}	0.59 ± 0.01^{e}	0.19 ± 0.02^{bc}	0.00
	4 h	3.81 ± 0.02^{bc}	0.26 ± 0.01^{b}	1.07 ± 0.01^{b}	82.34 ± 0.48^{a}	12.61 ± 0.07^{e}	5.07 ± 0.03^{b}	0.00	0.00

* Different lowercase letters indicate significant differences within the same column ($p < 0.05$, Tukey HSD).

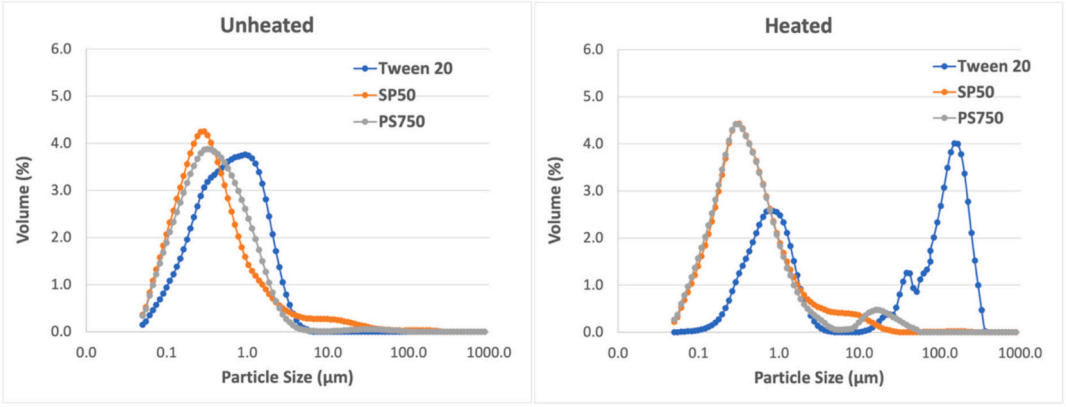

Fig. 1. Comparison of emulsifier behaviors in unheated and heated (100 °C for 4 h) emulsion systems.

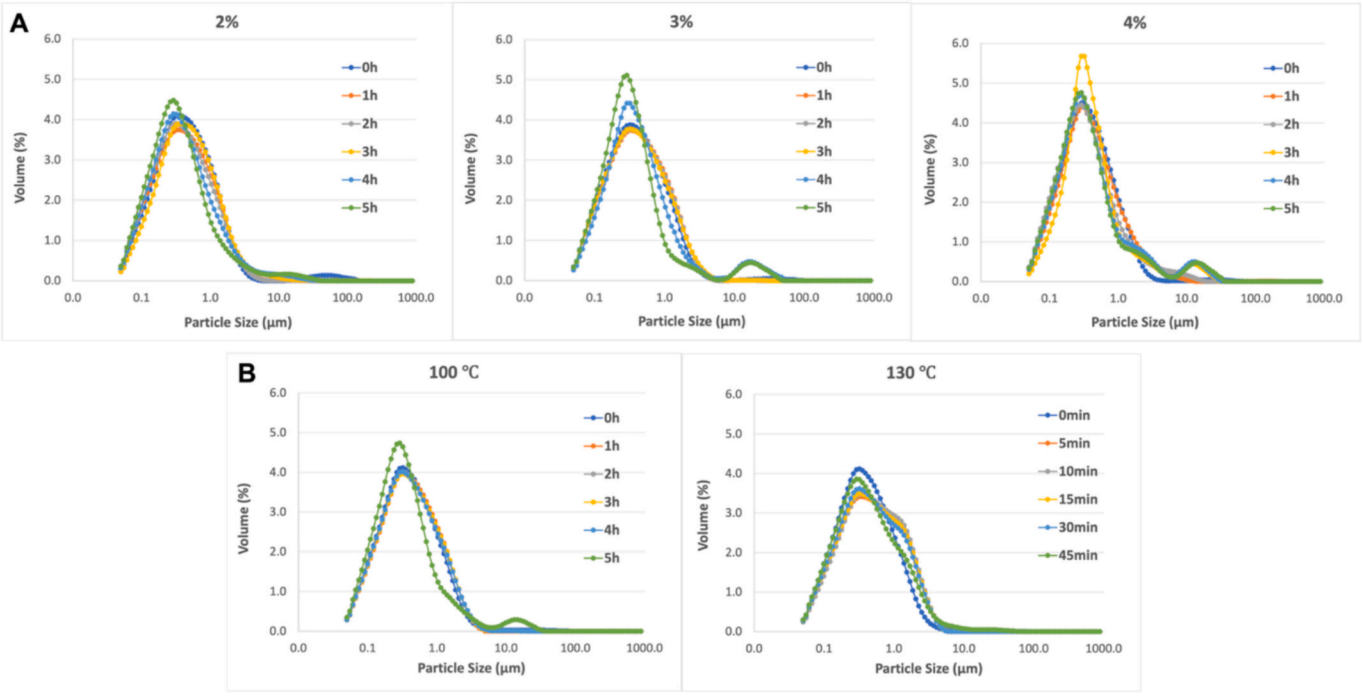

Fig. 2. A. The particle size distribution of emulsions prepared with 2%, 3% and 4% of sucrose ester and 10% of canola oil during heating over 5 h at 100 °C. **B.** Particle size distribution of emulsions containing ribose and cysteine prepared with 3% of sucrose ester and 10% of canola oil during heating over 5 h at 100 °C, and 45 min at 130 °C.

no phase separation observed for both unheated and heated samples over 20 days (Table S2, Fig. S4A). At 40 °C, emulsions containing 2% sucrose ester (PS750) formed a creamy emulsion phase after 7 days, whereas emulsions with higher sucrose ester concentrations (3% and 4%) separated after 10 days (Fig. 3A) due to heat-induced separation during storage (McClements & Jafari, 2018). This difference might be associated with the lower emulsifier concentration in the emulsion containing 2% sucrose ester, which resulted in lower viscosity and early phase separation compared to emulsions containing 3% and 4% sucrose ester (Fig. 4). Higher viscosity could improve emulsion stability by reducing droplet mobility according to Stokes' law (McClements & Jafari, 2018). However, the viscosity of the emulsions decreased markedly after heating, which could be attributed to the structural changes induced during the heating process (Fig. 4) (Petelin et al., 2025).

As shown in Fig. 3B, the heated emulsion prepared with Tween 20 formed a creamy layer at the surface after 2 days at 4 °C, 20 °C, and 40 °C, and this layer gradually increased over the 20-day storage period. In contrast, the unheated Tween 20 emulsion was stable at 4 °C and 20 °C, yet underwent phase separation after 7 days at 40 °C. Similar to sucrose ester-based emulsions, the extent of creaming was strongly affected by storage temperature.

Two distinct separation behaviors were observed depending on the emulsifier used during storage at 40 °C (Fig. S4B) after 20 days. In the sucrose ester-stabilized emulsion (both unheated and heated), phase separation occurred in the form of a creamy emulsion layer and an aqueous phase. During the initial storage time (after 7 and 10 days), the emulsion cream layer started to appear and tended to decrease or did not change at prolonged storage time (up to 20 days) (Fig. 3A). This reduction could be explained by the collapse and compaction of the cream layer through droplet coalescence and subsequent oil release (Mohd Isa et al., 2021). This might suggest a transition from reversible creaming to irreversible emulsion breakdown, rather than an improvement in emulsion stability. On the other hand, heated Tween 20-stabilized emulsions formed a cream layer after 2 days, leading to irreversible destabilization with the appearance of free oil after 20 days

Table 2
Particle size characterization of emulsions made using 2%, 3% and 4% of sucrose ester (PS750) and 10% of canola oil before and during heating at 100 °C for 5 h, and emulsions containing ribose and cysteine (P) with 3% of sucrose ester and 10% canola oil at 100 °C for 5 h and at 130 °C for 45 min.*

						% Volume fraction				
Emulsifier concentration (%)	**Temperature**	**Time**	**Span value**	**$D_{3,2}$ (μm)**	**$D_{4,3}$ (μm)**	**0.1–1 μm**	**1–10 μm**	**10–50 μm**	**50–100 μm**	**100–1000 μm**
2%	100 °C	0 h	3.20 ± 0.02^{c}	0.30 ± 0.01^{a}	1.83 ± 0.05^{a}	80.97 ± 0.45^{cd}	17.05 ± 0.86^{ab}	0.99 ± 0.05^{ab}	0.83 ± 0.04^{a}	0.17 ± 0.01^{a}
		1 h	3.30 ± 0.11^{bc}	0.28 ± 0.01^{a}	0.67 ± 0.04^{b}	81.53 ± 0.36^{bcd}	18.38 ± 0.36^{ab}	0.09 ± 0.01^{b}	0.00	0.00
		2 h	3.32 ± 0.05^{bc}	0.27 ± 0.01^{a}	0.63 ± 0.03^{b}	83.17 ± 0.76^{bc}	16.76 ± 0.74^{ab}	0.08 ± 0.01^{b}	0.00	0.00
		3 h	3.26 ± 0.11^{c}	0.31 ± 0.02^{a}	0.98 ± 0.23^{b}	78.85 ± 0.29^{d}	20.60 ± 0.64^{a}	0.76 ± 0.33^{ab}	0.05 ± 0.01^{b}	0.03 ± 0.01^{b}
		4 h	4.08 ± 0.15^{a}	0.27 ± 0.01^{a}	0.93 ± 0.15^{b}	82.77 ± 0.77^{ab}	16.15 ± 0.36^{b}	1.02 ± 0.21^{ab}	0.04 ± 0.01^{b}	0.00
		5 h	3.80 ± 0.04^{ab}	0.25 ± 0.01^{a}	0.90 ± 0.15^{b}	86.27 ± 0.11^{a}	12.21 ± 0.01^{c}	1.52 ± 0.16^{a}	0.00	0.00
3%	100 °C	0 h	3.23 ± 0.03^{b}	0.26 ± 0.01^{a}	0.81 ± 0.09^{bc}	83.83 ± 0.08^{b}	15.37 ± 0.77^{a}	0.59 ± 0.03^{c}	0.19 ± 0.01^{a}	0.00
		1 h	3.46 ± 0.20^{ab}	0.26 ± 0.02^{a}	0.68 ± 0.03^{bc}	81.57 ± 0.07^{b}	18.34 ± 0.91^{a}	0.10 ± 0.01^{c}	0.00	0.00
		2 h	3.47 ± 0.15^{ab}	0.28 ± 0.01^{a}	0.73 ± 0.09^{bc}	81.89 ± 0.05^{b}	18.06 ± 0.05^{a}	0.07 ± 0.01^{c}	0.00	0.00
		3 h	3.44 ± 0.06^{ab}	0.27 ± 0.01^{a}	0.66 ± 0.02^{c}	81.91 ± 0.59^{b}	18.00 ± 0.56^{a}	0.10 ± 0.01^{c}	0.00	0.00
		4 h	3.81 ± 0.02^{ab}	0.26 ± 0.01^{a}	1.07 ± 0.01^{ab}	82.33 ± 0.82^{b}	12.61 ± 0.58^{b}	5.06 ± 0.13^{a}	0.00	0.00
		5 h	3.92 ± 0.02^{a}	0.25 ± 0.01^{a}	1.41 ± 0.11^{a}	88.47 ± 0.34^{a}	6.91 ± 0.11^{c}	4.60 ± 0.44^{ab}	0.02 ± 0.01^{b}	0.00
3% (P)	100 °C	0 h	3.21 ± 0.06^{b}	0.27 ± 0.01^{ab}	0.82 ± 0.07^{ab}	83.99 ± 0.59^{ab}	15.49 ± 0.11^{b}	0.45 ± 0.02^{b}	0.04 ± 0.01^{a}	0.00
		1 h	3.23 ± 0.04^{ab}	0.29 ± 0.01^{a}	0.65 ± 0.02^{b}	82.16 ± 0.56^{b}	17.85 ± 0.12^{a}	0.00	0.00	0.00
		2 h	3.22 ± 0.06^{ab}	0.28 ± 0.01^{ab}	0.65 ± 0.01^{b}	82.32 ± 0.60^{b}	17.64 ± 0.14^{a}	0.04 ± 0.01^{c}	0.00	0.00
		3 h	3.25 ± 0.02^{ab}	0.28 ± 0.01^{ab}	0.64 ± 0.01^{b}	82.09 ± 0.43^{b}	17.89 ± 0.13^{a}	0.04 ± 0.01^{c}	0.00	0.00
		4 h	3.48 ± 0.24^{ab}	0.28 ± 0.01^{ab}	0.64 ± 0.01^{b}	82.39 ± 0.57^{b}	17.56 ± 0.10^{a}	0.05 ± 0.01^{c}	0.00	0.00
		5 h	3.92 ± 0.05^{a}	0.24 ± 0.01^{b}	0.98 ± 0.09^{a}	86.83 ± 0.61^{a}	10.83 ± 0.01^{c}	2.33 ± 0.07^{a}	0.00	0.00
	130 °C	0 min	3.21 ± 0.06^{c}	0.27 ± 0.01^{a}	0.82 ± 0.07^{a}	83.99 ± 0.62^{a}	15.49 ± 0.12^{e}	0.45 ± 0.01^{b}	0.04 ± 0.01^{a}	0.00
		5 min	3.53 ± 0.16^{c}	0.27 ± 0.02^{a}	0.83 ± 0.17^{a}	74.46 ± 0.56^{c}	25.52 ± 0.19^{ab}	0.00	0.00	0.00
		10 min	3.74 ± 0.01^{c}	0.25 ± 0.01^{a}	0.71 ± 0.04^{a}	73.71 ± 0.45^{c}	26.31 ± 0.20^{a}	0.00	0.00	0.00
		15 min	4.32 ± 0.54^{bc}	0.30 ± 0.05^{a}	1.16 ± 0.25^{a}	74.89 ± 0.57^{c}	25.11 ± 0.18^{ab}	0.00	0.00	0.00
		30 min	5.78 ± 0.25^{a}	0.26 ± 0.01^{a}	1.27 ± 0.02^{a}	76.05 ± 0.38^{bc}	23.96 ± 0.16^{c}	0.00	0.00	0.00
		45 min	5.70 ± 0.05^{ab}	0.25 ± 0.01^{a}	1.32 ± 0.01^{a}	78.58 ± 0.61^{b}	20.61 ± 0.23^{d}	0.74 ± 0.01^{a}	0.02 ± 0.01^{b}	0.00
4%	100 °C	0 h	2.86 ± 0.03^{c}	0.26 ± 0.01^{a}	0.70 ± 0.05^{a}	88.12 ± 0.44^{a}	11.27 ± 0.12^{c}	0.59 ± 0.01^{d}	0.04 ± 0.01^{a}	0.00
		1 h	3.53 ± 0.16^{bc}	0.27 ± 0.02^{a}	0.83 ± 0.17^{a}	84.17 ± 0.34^{bc}	15.68 ± 0.16^{a}	0.05 ± 0.02^{f}	0.02 ± 0.01^{b}	0.08 ± 0.01^{a}
		2 h	3.74 ± 0.01^{abc}	0.25 ± 0.01^{a}	0.71 ± 0.04^{a}	86.39 ± 0.45^{ab}	13.16 ± 0.14^{b}	0.43 ± 0.01^{e}	0.00	0.00
		3 h	4.32 ± 0.54^{abc}	0.30 ± 0.05^{a}	1.16 ± 0.25^{a}	85.22 ± 0.24^{bc}	11.73 ± 0.15^{c}	3.04 ± 0.01^{c}	0.00	0.00
		4 h	5.78 ± 0.25^{ab}	0.26 ± 0.01^{a}	1.27 ± 0.02^{a}	82.99 ± 0.42^{c}	13.40 ± 0.20^{b}	3.61 ± 0.03^{b}	0.00	0.00
		5 h	5.70 ± 0.05^{a}	0.25 ± 0.01^{a}	1.32 ± 0.01^{a}	84.555 ± 0.38^{bc}	11.45 ± 0.10^{c}	3.96 ± 0.05^{a}	0.00	0.00

* Different lowercase letters indicate significant differences within the same column between temperatures for each emulsion model separately ($p < 0.05$, Tukey HSD).

at 40 °C, while no free oil was observed at 4 °C or 20 °C over 20 days (Fig. 3B and Fig. S4B-C). Therefore, sucrose ester generally showed better emulsion stability across different storage temperatures compared to Tween 20, in agreement with particle size measurements of heated emulsions prepared with Tween 20 and PS750 (Fig. 1).

3.2.3. Surface and interfacial tensions

As shown in Table 3, interfacial tension between canola oil and water was 24.2 ± 1.4 mN/m and it decreased when emulsifiers were introduced to the system as expected. It was known that an emulsifier was able to reduce the interfacial tension between bulk oil and water phase by creating smaller droplets. Due to having both hydrophobic and hydrophilic sites, Tween 20 and PS750 sucrose ester reduced the interfacial

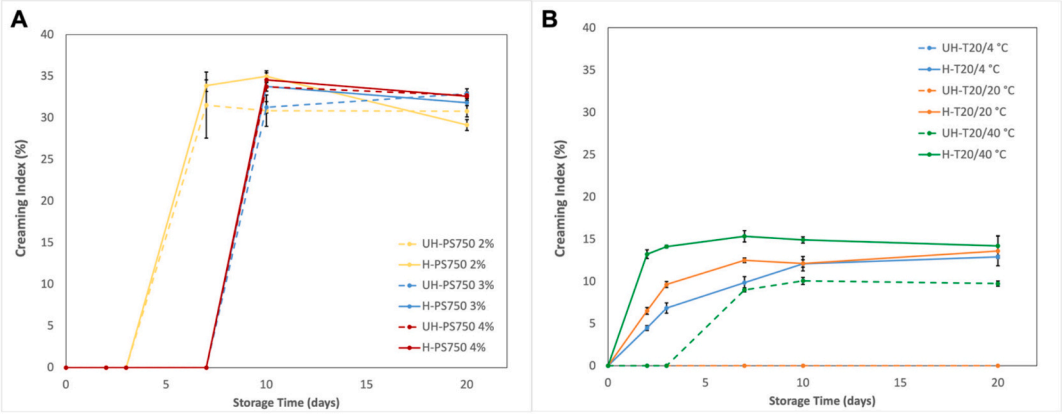

Fig. 3. A. The creaming index (%) of unheated (UH) and heated (H) emulsions prepared with PS750 (2%, 3%, and 4%) during storage at 40 °C for 20 days. **B.** Creaming index (%) of unheated (UH) and heated (H) emulsions prepared with Tween 20 (T20, 3%) during storage at 4 °C, 20 °C, and 40 °C for 20 days.

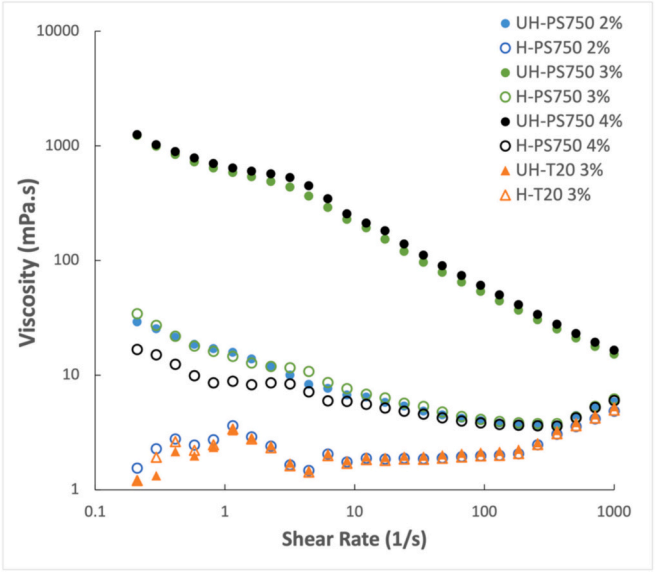

Fig. 4. Viscosity of unheated (UH) and heated (H) emulsions prepared with PS750 (2%, 3% and 4%) and Tween 20 (T20, 3%) at 20 °C.

Table 3
Surface tension between different phases and interfacial tension between canola oil and water, and between canola oil and corresponding emulsifier solutions in water.*

	Surface tension (mN/m)
Water (Air)	73.2 ± 0.4[a]
Canola oil (Air)	37.7 ± 0.9[b]
	Interfacial tension (mN/m)
Water (Canola oil)	24.2 ± 1.4[c]
Tween 20 (3%)	3.7 ± 0.4[d]
PS750 (3%)	1.3 ± 0.1[e]

* Different lowercase letters indicate significant differences within the same column ($p < 0.05$, Tukey HSD).

tension between canola oil and water to 3.7 ± 1.0 mN/m and 1.3 ± 0.1 mN/m, respectively. As control measurements, surface tension between water and air was 73 ± 0.4 mN/m, and between canola oil and air was 37.7 ± 0.9 mN/m, in accordance with previous studies (Sahasrabudhe et al., 2017) (Pérez-Díaz et al., 2012).

Emulsifier absorption at the interface was associated with emulsifier monomer availability in the continuous phase to create emulsion droplets (McClements & Jafari, 2018). CMC was defined as the concentration at which emulsifier monomers in the continuous phase begin to form self-assembly micelles. In Fig. 5, it was observed that PS750 sucrose ester and Tween 20 reduced the surface tension between water and air from 73.2 ± 0.4 mN/m to 31.9 ± 0.4 mN/m, and 37.7 ± 0.2 mN/m, respectively. CMC was observed as 0.002% for PS750 and 0.01% for Tween 20, in which PS750 sucrose ester was able to reduce the surface tension at lower concentration (%), compared to Tween 20.

3.3. Formation of thiol compounds

The volatile compounds containing free thiol groups were studied in four different systems, as emulsion (87% buffer, 10% canola oil and 3% emulsifier), buffer/oil (90% buffer and 10% canola oil), buffer/emulsifier (97% buffer and 3% emulsifier) and buffer alone, after heating at 100 °C, 110 °C, 120 °C and 130 °C for 4 h, 2 h, 1 h and 0.5 h, respectively (Fig. 6). These heating times were selected with respect to the breaking points of the emulsion at lower temperature/longer time and at higher temperature/shorter time combinations obtained from particle size behaviors during heating. In general, heating at lower temperatures for

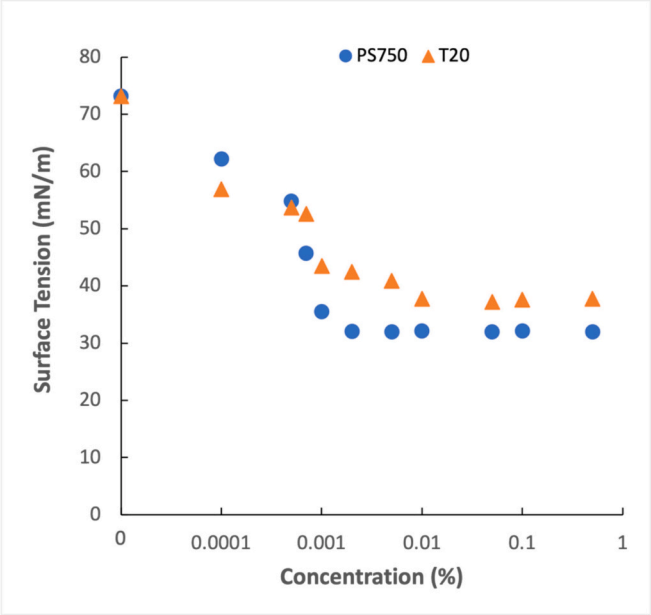

Fig. 5. Surface tension *versus* concentration graph of PS750 and Tween 20 (T20).

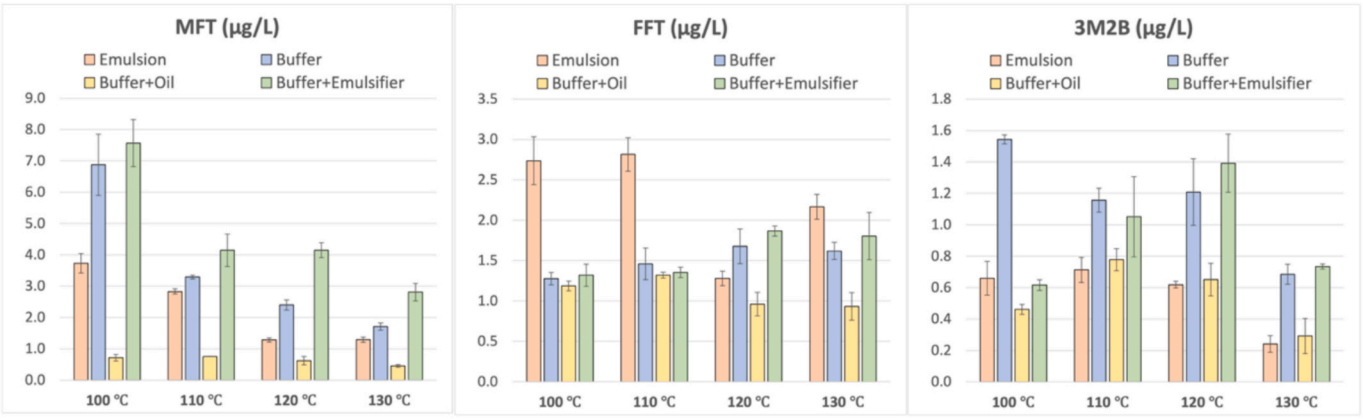

Fig. 6. The formation of 2-methyl-3-furanthiol (MFT), 2-furfurylthiol (FFT), and 3-mercapto-2-butanone (3M2B) in model systems after heating for 4 h, 2 h, 1 h and 0.5 h at 100 °C, 110 °C, 120 °C and 130 °C, respectively.

longer times led to increased MFT, FFT, and 3M2B formations. In emulsion model systems, a decreasing trend in thiol compounds was observed as the heating temperature increased and the heating time decreased. The formation of thiol compounds was higher in the models without oil compared to the models with oil, whereas emulsifier mostly increased the amount of thiol compounds, compared to the models without emulsifier ($p < 0.05$).

One of the major steps for aroma generation in the Maillard reaction is Strecker degradation where dicarbonyl compounds formed from Amadori or sugar degradation products condense with amino acids (Eskin et al., 2013; Hellwig et al., 2018). Cysteine, having a mercapto group, has a particular importance in meat aroma development, as after Strecker degradation it provides hydrogen sulfide, which is essential for the formation of potent savory and meaty thiols such as MFT, FFT and mercaptoketones (Whitfield & Mottram, 1999; Yeo et al., 2022). Early investigations proposed that MFT was formed from the reaction between 4-hydroxy-5-methyl-3(2*H*)-furanone (norfuraneol), a major degradation product of pentoses, and hydrogen sulfide (Mottram & Whitfield, 1993; Whitfield & Mottram, 1999). On the other hand, a reaction system containing labeled ribose and unlabeled cysteine showed that norfuraneol did not show a significant impact on the generation of MFT, but instead, 1,4-dideoxyosone was proposed to explain MFT formation (Cerny & Davidek, 2003). Additionally, another route was reported when MFT was formed from hydroxyacetaldehyde and 1-mercapto-2-propanone; again, it was not associated with norfuraneol (Hofmann & Schieberle, 1998). In these studies, furfural formed from pentoses was considered as a crucial intermediate to yield FFT. Similarly, mercaptoketones such as 3M2B were detected in meaty reaction mixtures as an intermediate product contributing to the overall aroma profile, formed through the reaction between α-dicarbonyl compounds and hydrogen sulfide (Cerny & Davidek, 2003; Yeo et al., 2022).

The formation of MFT was highest during heating at 100 °C for 4 h, reaching 6.88 ± 0.98 µg/L and 7.57 ± 0.75 µg/L in buffer and buffer/emulsifier system, respectively, and decreased by 75% and 63% after heating at 130 °C for 0.5 h ($p < 0.05$). A similar trend was observed in the emulsion and buffer/oil system, with the highest MFT formation at 100 °C for 4 h, and reduced by 65% and 38% when heated at 130 °C for 0.5 h ($p < 0.05$). This could be attributed to the acceleration of the Maillard reaction and lipid degradation, where reactive intermediates leading to the formation of thiol compounds tend to compete with each other more readily during high temperature heating (Lund & Ray, 2017). Additionally, the amount of MFT was limited in heated buffer/oil system compared to the other systems, because lipid oxidation products such as unsaturated aldehydes and other carbonyl compounds generated during heating could modify the Maillard reaction route by reacting with hydrogen sulfide, leading to limited formation of thiol compounds (Bleicher et al., 2022). Although the emulsion (*i.e.*, emulsifier/buffer/oil system) and the buffer/oil system contained the same oil content (10%), the relative concentration of hexanal, as a lipid oxidation marker (Bleicher et al., 2022), increased significantly in the emulsion compared to the other systems across all temperature-time combinations (Fig. S5). Furthermore, the amount of MFT in the emulsion was 5.1-, 3.8-, 2.1- and 2.9-fold higher than in the buffer/oil system after heating at 100 °C, 110 °C, 120 °C and 130 °C for 4 h, 2 h, 1 h and 0.5 h, respectively ($p < 0.05$). The enhanced formation of meaty compounds in the emulsion may be attributed to its structure, as the sucrose ester emulsifier lowered interfacial tension (Table 3), resulting in smaller droplets and a larger interfacial area. It was reported that the formation of MFT was enhanced by the cubic phase structure of an emulsion formed by monoglycerides due to its very large interface (400 m^2/g), while it was not detected in an aqueous model after heating at 100 °C for 4 h under acidic conditions (pH 5.0) (Vauthey et al., 2000). Additionally, partitioning of MFT at the interface of the emulsion structure possibly increased the concentration of MFT, since the lipid domain prevented its degradation compared to the aqueous domain. Moreover, it was proposed that compartmentalization of the reactants due to partitioning resulted in local accumulation on the droplet surface. Higher concentration at the interface produced a gradient that led to an increase in the reaction rates (Yaghmur et al., 2005). Furthermore, generated compounds could also accumulate and be protected at the interface during heating.

As the octanol/water partition coefficient (Log P) and pH-dependent distribution coefficient (Log D) are important for particle localization, it is generally accepted that micelle structures can retain molecules with partition coefficients between −0.5 and 2 at the interface. On the other hand, values below −0.5 and above 2 tend to have low lipophilicity or low hydrophilicity, respectively (Kwon, 2002). Considering MFT partitioning at pH 5.5 (Log $D_{5.5}$) is 1.94 and Log P is 2.14 (predictive data from ACD PhysChem Suite (Advanced Chemistry Development, Inc., Toronto, ON, Canada)), MFT tended to locate closer to the interface and the lipid domain rather than the aqueous domain and was probably protected from further reactions. However, cysteine and ribose were likely to be located in the water domain under acidic conditions because their Log $D_{5.5}$ values are −2.50 and − 2.09. But one of the proposed precursors for MFT, 1-mercapto-2-propanone has Log $D_{5.5}$ value of 0.51 (and 0.32 Log *P* value), indicating that it could accumulate at the interface. In a model system of self-assembly structured fluids (mesophases) prepared with xylose and glycine or leucine, it was found that the interface could protect the intermediate, namely norfuraneol, and resulted in its accumulation after heating at 70 °C and pH 6.0 (Blank et al., 2006). Norfuraneol has a Log $D_{6.0}$ value of −0.09 (Log $D_{5.5}$ = −0.08) and tends to locate at the interface and close to the water domain. Similarly, a self-assembled water-in-oil reversed microemulsion (reversed micelles vehicles) created by monoglycerides containing soya bean oil with cysteine and xylose had 60 times higher MFT than the

phosphate buffer system containing the same precursors, after heating at 95 °C for 2 h (Sagalowicz et al., 2016). Finally, emulsifiers could form a micelle structure and act as an emulsion droplet in the absence of oil which might induce the formation of glycation reactions and Strecker degradation at higher temperatures (Troise et al., 2016; Troise, Fogliano, et al., 2020). This might explain why the buffer/emulsifier system promoted the formation of MFT compared to buffer system alone. Emulsifier micelles possibly provided a more hydrophobic reaction environment compared to the buffer system, where compartmentalization occurred even in the absence of vegetable oil (Ullrich et al., 2008; Virdi et al., 2024). This resulted in a higher production of thiol compounds without modifications from unsaturated oil.

It should be noted that the precursors used for meaty aroma formation in the studies mentioned above (Blank et al., 2006; Sagalowicz et al., 2016) were almost 10 times higher than in the current study, and higher amounts of MFT were generated in emulsion models compared to buffer models, contrary to the current study. Furthermore, the lipid degradation in canola oil may vary from that of a saturated monoglycerides/soya bean oil mixture (2:1, *w/w*) during heating, due to differences in unsaturation levels (Elmore & Mottram, 2006). This could influence the formation of MFT in various ways.

Unlike the generation of MFT, where its concentration was higher in the oil-free systems, the maximum formation of FFT was found in emulsion models as 2.74 ± 0.3 μg/L and 2.81 ± 0.21 μg/L after heating at 100 °C for 4 h and at 110 °C for 2 h, respectively. Moreover, FFT formation tended to increase in buffer and buffer/emulsion systems up to 1.68 ± 0.21 μg/L and 1.87 ± 0.06 μg/L with increasing heating temperature and decreasing time. FFT formation was not as adversely affected as MFT formation in model systems containing oil compared to non-oil model systems, in agreement with previous studies (Elmore et al., 2002; Van Ba et al., 2013; Xu et al., 2011). This could be attributed to there being different formation mechanisms for FFT and MFT (Parker, 2017). In general, FFT content was lower than MFT, especially at 100 °C for 4 h. On the other hand, the amount of FFT was between 0.93 ± 0.17 and 1.19 ± 0.06 in buffer/oil system heated at the studied temperature/time combinations, which was higher than MFT. Comparing heating at 100 °C for 4 h to 130 °C for 0.5 h, FFT generation was reduced by 21% in both emulsion and buffer/oil systems whereas 27% more FFT was formed in both buffer and buffer/emulsifier systems ($p < 0.05$). These results were in line with reports that FFT generation was promoted by emulsion structures compared to control buffer models (Yaghmur et al., 2002, 2005). This was explained by the same phenomena that occurred during MFT formation, *i.e.*, compartmentalization and regioselectivity of precursors and FFT. The formation of FFT, and the conversion rate of furfural to FFT, were significantly higher in a microemulsion prepared with R-(+)-limonene than in an aqueous model at 65 °C and pH 5.0 (Yaghmur et al., 2002, 2005). Comparable with MFT, FFT having a Log $D_{5.5}$ value of 1.88 and furfural having a Log $D_{5.5}$ value of 0.69 could be located at the interface and also in the lipid domain.

The amount of 3M2B was lower in relation to MFT and FFT: it ranged from 0.24 ± 0.05 μg/L to 1.54 ± 0.03 μg/L, probably due to a lower rate of formation during heating and/or due to participation in further reactions as a reactive intermediate. The models containing oil were less favorable in accumulating 3M2B compared to the oil-free systems, especially during heating at 130 °C for 0.5 h, while heating at 120 °C for 1 h showed a positive effect on 3M2B formation in buffer and buffer/emulsifier systems.

4. Conclusion

This study investigated the physicochemical characterization of emulsions formulated with different emulsifiers before and after heat treatment. This study also evaluated the formation of MFT, FFT and 3M2B as potent thiol compounds in heated emulsion systems containing cysteine and ribose (buffer/canola oil/sucrose ester) and in corresponding control systems (buffer, buffer/canola oil and buffer/sucrose ester). Samples were subjected to thermal processing at 100 °C for 4 h, 110 °C for 2 h, 120 °C for 1 h and 130 °C for 0.5 h, to induce aroma formation through the Maillard reaction.

After heating at 100 °C for 4 h, all emulsion models prepared with sucrose ester (PS750) remained highly stable during storage at 4 °C and 20 °C for 20 days, while storage under accelerated conditions at 40 °C promoted phase separation over 20 days. The emulsion prepared with Tween 20 exhibited insufficient stability during storage at 4 °C and 20 °C after heating at 100 °C for 4 h and formed a free oil layer during storage at 40 °C, mainly due to an increase in larger droplet volumes leading to droplet coalescence.

The formation of potent aroma compounds, namely MFT, FFT, and 3M2B, was affected by both heating temperature and time. Lower temperatures and longer times for heating induced the generation of MFT and FFT, whereas higher temperatures and shorter times restricted the accumulation of thiol compounds. Although a lipid oxidation marker (hexanal) increased in emulsions with canola oil, the formation of MFT and FFT was enhanced during heating at 100 °C for 4 h, due to the larger surface area of emulsion droplets with respect to the buffer/oil system. This larger interfacial area was created as a result of the reduction in the interfacial tension between canola oil and water from 24.2 ± 1.4 mN/m to 1.3 ± 0.1 mN/m by the sucrose ester (PS750).

The results revealed that it is possible to create highly heat-stable emulsions with sucrose esters without using supportive components such as polar lipids or alcohols. This research highlights the critical role of emulsifier and heat treatment parameters in the generation of potent thiol aroma compounds, particularly within the studied emulsion system. Emulsion and emulsifier interfaces might help to generate powerful top notes for plant-based products, providing a cost-effective approach and meeting consumer expectations.

CRediT authorship contribution statement

Suleyman Yiltirak: Writing – review & editing, Writing – original draft, Validation, Methodology, Investigation, Formal analysis, Data curation, Conceptualization. **Dimitris P. Balagiannis:** Writing – review & editing, Supervision, Project administration, Methodology, Conceptualization. **Jan Koek:** Writing – review & editing, Visualization, Supervision, Project administration, Conceptualization. **Jens Koch:** Writing – review & editing, Supervision, Project administration, Conceptualization. **J. Stephen Elmore:** Writing – review & editing, Supervision, Project administration, Methodology, Funding acquisition, Conceptualization.

Funding

Suleyman Yiltirak was funded by the Biotechnology and Biological Sciences Research Council (BBSRC), and industrial sponsors Unilever and Symrise AG, through UKRI BBSRC Collaborative Training Partnership (Grant ref. BB/W510592/1).

Declaration of competing interest

The authors declare that they have no known competing financial interests or personal relationships that could have appeared to influence the work reported in this paper.

Acknowledgment

We are grateful to industrial supervisors Donny Merkx from Unilever and Christopher Sabater from Symrise AG for their support.

Appendix A. Supplementary data

Supplementary data to this article can be found online at https://doi.org/10.1016/j.foodres.2026.118600.

Data availability

Data will be made available on request.

References

Ahmad, M., Qureshi, S., Akbar, M. H., Siddiqui, S. A., Gani, A., Mushtaq, M., … Dhull, S. B. (2022). Plant-based meat alternatives: Compositional analysis, current development and challenges. *Applied Food Research, 2*(2), Article 100154. https://doi.org/10.1016/j.afres.2022.100154

André, M. V., Alves, V. D., Prista, C., Martins, L. L., Mota, M., Mourato, M. P., … Matos, T. J. S. (2025). Nutritional traits and physicochemical parameters of dry aged-in-bag and cooked serpentina goat meat. *Food Science & Nutrition, 13*(9), Article e70538. https://doi.org/10.1002/fsn3.70538

Appiani, M., Cattaneo, C., & Laureati, M. (2023). Sensory properties and consumer acceptance of plant-based meat, dairy, fish and eggs analogs: A systematic review. *Frontiers in Sustainable Food Systems, 7*. https://doi.org/10.3389/fsufs.2023.1268068

Blank, I., Davidek, T., Devaud, S., Sagalowicz, L., Leser, M. E., & Michel, M. (2006). Formation of 4-hydroxy-5-methyl-3(2H)-furanone (norfuraneol) in structured fluids. In W. L. P. Bredie, & M. A. Petersen (Eds.), *43. Flavour Science* (pp. 347–350). Elsevier. https://doi.org/10.1016/S0167-4501(06)80082-8.

Bleicher, J., Ebner, E. E., & Bak, K. H. (2022). Formation and analysis of volatile and odor compounds in meat—A review. *Molecules, 27, 19*, 6703. https://doi.org/10.3390/molecules27196703

Capone, D. L., Sefton, M. A., & Jeffery, D. W. (2011). Application of a modified method for 3-Mercaptohexan-1-ol determination to investigate the relationship between free thiol and related conjugates in grape juice and wine. *Journal of Agricultural and Food Chemistry, 59*(9), 4649–4658. https://doi.org/10.1021/jf200116q

Cerny, C. (2012). Savory Flavors. In *Handbook of meat, poultry and seafood quality* (pp. 105–126). Ltd: John Wiley & Sons. https://doi.org/10.1002/9781118352434.ch8.

Cerny, C., & Davidek, T. (2003). Formation of aroma compounds from ribose and cysteine during the Maillard reaction. *Journal of Agricultural and Food Chemistry, 51*(9), 2714–2721. https://doi.org/10.1021/jf026123f

Dunkel, A., Steinhaus, M., Kotthoff, M., Nowak, B., Krautwurst, D., Schieberle, P., & Hofmann, T. (2014). Nature's chemical signatures in human olfaction: A foodborne perspective for future biotechnology. *Angewandte Chemie International Edition, 53*(28), 7124–7143. https://doi.org/10.1002/anie.201309508

Elmore, J. S., Campo, M. M., Enser, M., & Mottram, D. S. (2002). Effect of lipid composition on meat-like model systems containing cysteine, ribose, and polyunsaturated fatty acids. *Journal of Agricultural and Food Chemistry, 50*(5), 1126–1132. https://doi.org/10.1021/jf0108718

Elmore, J. S., & Mottram, D. S. (2006). The role of lipid in the flavour of cooked beef. In W. L. P. Bredie & M. A. B. T.-D. in F. S. Petersen (Eds.), *Flavour Science* (Vol. 43, pp. 375–378). Elsevier. Doi: https://doi.org/10.1016/S0167-4501(06)80089-0.

Eskin, N. A. M., Ho, C.-T., & Shahidi, F. (2013). *Chapter 6 - Browning reactions in foods (N. A. M. Eskin & F. B. T.-B. Of F. (third E. Shahidi, eds.; pp. 245–289)). Academic press*. https://doi.org/10.1016/B978-0-08-091809-9.00006-6

Fanun, M., Leser, M., Aserin, A., & Garti, N. (2001). Sucrose ester microemulsions as microreactors for model Maillard reaction. *Colloids and Surfaces A: Physicochemical and Engineering Aspects, 194*(1), 175–187. https://doi.org/10.1016/S0927-7757(01)00786-5

Feng, J., Berton-Carabin, C. C., Fogliano, V., & Schroën, K. (2022). Maillard reaction products as functional components in oil-in-water emulsions: A review highlighting interfacial and antioxidant properties. *Trends in Food Science & Technology, 121*, 129–141. https://doi.org/10.1016/j.tifs.2022.02.008

Ghazani, S. M., & Marangoni, A. G. (2016). Healthy fats and oils. *Elsevier*. https://doi.org/10.1016/B978-0-08-100596-5.00100-1

Giles, H., Bull, S. P., Lignou, S., Gallagher, J., Faka, M., Rodriguez-Garcia, J., & Methven, L. (2025). Co-spray drying whey protein isolate with polysaccharides provides additional lubrication impacting the sensory profile of model beverages. *Food Hydrocolloids, 160*, Article 110778. https://doi.org/10.1016/j.foodhyd.2024.110778

Hellwig, M., Gensberger-Reigl, S., Henle, T., & Pischetsrieder, M. (2018). Food-derived 1,2-dicarbonyl compounds and their role in diseases. *Seminars in Cancer Biology, 49*(March 2017), 1–8. https://doi.org/10.1016/j.semcancer.2017.11.014

Hofmann, T., & Schieberle, P. (1995). Evaluation of the key odorants in a thermally treated solution of ribose and cysteine by aroma extract dilution techniques. *Journal of Agricultural and Food Chemistry, 43*(8), 2187–2194. https://doi.org/10.1021/jf00056a042

Hofmann, T., & Schieberle, P. (1998). Quantitative model studies on the effectiveness of different precursor Systems in the Formation of the intense food odorants 2-furfurylthiol and 2-Methyl-3-furanthiol. *Journal of Agricultural and Food Chemistry, 46*(1), 235–241. https://doi.org/10.1021/jf9705983

International Council for Harmonisation of Technical Requirements for Pharmaceuticals for Human Use. (2023). *ICH Q2(R2): Guideline on validation of analytical procedures (step 5)*. Geneva, Switzerland: ICH.

Kampa, J., Frazier, R., & Rodriguez-Garcia, J. (2022). Physical and chemical characterisation of conventional and Nano/emulsions: Influence of vegetable oils from different origins. *Foods, 11*(5). https://doi.org/10.3390/foods11050681

Kampa, J., Koidis, A., Ghawi, S. K., Frazier, R. A., & Rodriguez-Garcia, J. (2022). Optimisation of the physicochemical stability of extra virgin olive oil-in-water nanoemulsion: Processing parameters and stabiliser type. *European Food Research and Technology, 248*(11), 2765–2777. https://doi.org/10.1007/s00217-022-04088-7

Kwon, Y. (Ed.). (2002). *Absorption BT - Handbook of essential pharmacokinetics, pharmacodynamics and drug metabolism for industrial scientists* (pp. 35–72). US: Springer. https://doi.org/10.1007/0-306-46820-4_4.

Lund, M. N., & Ray, C. A. (2017). Control of Maillard reactions in foods: Strategies and chemical mechanisms. *Journal of Agricultural and Food Chemistry, 65*(23), 4537–4552. https://doi.org/10.1021/acs.jafc.7b00882

Lutz, R. A. A., & Garti, N. (2005). Maillard reaction between leucine and glucose in O/W microemulsion Media in Comparison to aqueous solution. *Journal of Dispersion Science and Technology, 26*(5), 535–547. https://doi.org/10.1081/DIS-200057627

McClements, D. J. (2004). Food emulsions: Principles, practices, and techniques. CRC press.

McClements, D. J., & Gumus, C. E. (2016). Natural emulsifiers — Biosurfactants, phospholipids, biopolymers, and colloidal particles: Molecular and physicochemical basis of functional performance. *Advances in Colloid and Interface Science, 234*, 3–26. https://doi.org/10.1016/j.cis.2016.03.002

McClements, D. J., & Jafari, S. M. (2018). Improving emulsion formation, stability and performance using mixed emulsifiers: A review. *Advances in Colloid and Interface Science, 251*, 55–79. https://doi.org/10.1016/j.cis.2017.12.001

Miao, X., Li, J., Li, S., Li, G., Dong, X., & Jiang, P. (2024). Exploring the impact of different processing techniques on quality and flavor characteristics in hoki steak soups. *Food Science & Nutrition, 12*, 10836–10847. https://doi.org/10.1002/fsn3.4616

Mohd Isa, N. S., El Kadri, H., Vigolo, D., & Gkatzionis, K. (2021). Optimisation of bacterial release from a stable microfluidic-generated water-in-oil-in-water emulsion. *RSC Advances, 11*, 7738–7749. https://doi.org/10.1039/D0RA10954A

Mottram, D. S., & Whitfield, F. B. (1993). Aroma volatiles from meat like Maillard systems. In *, Vol. 543. Thermally generated Flavors* (pp. 14–180). American Chemical Society. https://doi.org/10.1021/bk-1994-0543.ch014.

Parker, J. K. (2017). Meat. In A. Buettner (Ed.), *Springer Handbook of Odor* (pp. 29–30). Springer International Publishing. https://doi.org/10.1007/978-3-319-26932-0_10.

Pérez-Díaz, J. L., Álvarez-Valenzuela, M. A., & García-Prada, J. C. (2012). The effect of the partial pressure of water vapor on the surface tension of the liquid water–air interface. *Journal of Colloid and Interface Science, 381*(1), 180–182. https://doi.org/10.1016/j.jcis.2012.05.034

Petelin, R., Malvasio, M., Monetta, D., Rasia, M. C., Musumeci, M. A., & Benitez, L. O. (2025). Effects of different oils on the physiochemical properties of pea protein concentrate and maltodextrin emulsions. *Food and Bioprocess Technology, 18*, 5278–5293. https://doi.org/10.1007/s11947-025-03751-7

Rao, J., & McClements, D. J. (2011). Food-grade microemulsions, nanoemulsions and emulsions: Fabrication from sucrose monopalmitate & lemon oil. *Food Hydrocolloids, 25*(6), 1413–1423. https://doi.org/10.1016/j.foodhyd.2011.02.004

Sagalowicz, L., Leser, M. E., Watzke, H. J., & Michel, M. (2006). Monoglyceride self-assembly structures as delivery vehicles. *Trends in Food Science & Technology, 17*(5), 204–214. https://doi.org/10.1016/j.tifs.2005.12.012

Sagalowicz, L., Moccand, C., Davidek, T., Ghanbari, R., Martiel, I., Negrini, R., … Michel, M. (2016). Lipid self-assembled structures for reactivity control in food. *Philosophical Transactions. Series A, Mathematical, Physical, and Engineering Sciences, 374*(2072), 20150136. https://doi.org/10.1098/rsta.2015.0136

Sahasrabudhe, S. N., Rodriguez-Martinez, V., O'Meara, M., & Farkas, B. E. (2017). Density, viscosity, and surface tension of five vegetable oils at elevated temperatures: Measurement and modeling. *International Journal of Food Properties, 20*(sup2), 1965–1981. https://doi.org/10.1080/10942912.2017.1360905

van der Sluis, C., Hocquette, J.-F., & Chriki, S. (2026). Review: European consumers' attitudes towards the benefits of reducing meat consumption – The role of diverse and interconnected drivers. *Animal, 20*(1), Article 101718. https://doi.org/10.1016/j.animal.2025.101718

Troise, A. D., Berton-Carabin, C. C., & Fogliano, V. (2016). Amadori products formation in emulsified systems. *Food Chemistry, 199*, 51–58. https://doi.org/10.1016/j.foodchem.2015.11.110

Troise, A. D., Berton-Carabin, C. C., Vitaglione, P., & Fogliano, V. (2020). Formation of taste-active pyridinium betaine derivatives is promoted in thermally treated oil-in-water emulsions and alkaline pH. *Journal of Agricultural and Food Chemistry, 68*(18), 5180–5188. https://doi.org/10.1021/acs.jafc.0c01446

Troise, A. D., Fogliano, V., Vitaglione, P., & Berton-Carabin, C. C. (2020). Interrelated routes between the Maillard reaction and lipid oxidation in emulsion systems. *Journal of Agricultural and Food Chemistry, 68*(43), 12107–12115. https://doi.org/10.1021/acs.jafc.0c04738

Ullrich, S., Metz, H., & Mäder, K. (2008). Sucrose ester nanodispersions: Microviscosity and viscoelastic properties. *European Journal of Pharmaceutics and Biopharmaceutics, 70*(2), 550–555. https://doi.org/10.1016/j.ejpb.2008.05.014

Van Ba, H., Amna, T., & Hwang, I. (2013). Significant influence of particular unsaturated fatty acids and pH on the volatile compounds in meat-like model systems. *Meat Science, 94*(4), 480–488. https://doi.org/10.1016/j.meatsci.2013.04.029

Vauthey, S., Milo, C., Frossard, P., Garti, N., Leser, M. E., & Watzke, H. J. (2000). Structured fluids as microreactors for flavor formation by the Maillard reaction. *Journal of Agricultural and Food Chemistry, 48*(10), 4808–4816. https://doi.org/10.1021/jf991254a

Virdi, J. K., Dusunge, A., & Handa, S. (2024). Aqueous micelles as solvent, ligand, and reaction promoter in catalysis. *JACS Au, 4*(2), 301–317. https://doi.org/10.1021/jacsau.3c00605

Warner, A. (2024). Chef Anthony Warner on the high price of plant-based food. Food Manufacture. Retrieved from https://www.foodmanufacture.co.uk/Article/2024/02/19/chef-anthony-warner-on-the-high-price-of-plant-based-food/ (Accessed September 16, 2025).

Whitfield, F. B., & Mottram, D. S. (1999). Investigation of the reaction between 4-Hydroxy-5-methyl-3(2H)-furanone and cysteine or hydrogen Sulfide at pH 4.5. *Journal*

of Agricultural and Food Chemistry, 47(4), 1626–1634. https://doi.org/10.1021/jf980980v

Xu, Y., Chen, Q., Lei, S., Wu, P., Fan, G., Xu, X., & Pan, S. (2011). Effects of lard on the formation of volatiles from the Maillard reaction of cysteine with xylose. *Journal of the Science of Food and Agriculture, 91*(12), 2241–2246. https://doi.org/10.1002/jsfa.4445

Yaghmur, A., Aserin, A., Abbas, A., & Garti, N. (2005). Reactivity of furfural–cysteine model reaction in food-grade five-component nonionic O/W microemulsions. *Colloids and Surfaces A: Physicochemical and Engineering Aspects, 253*(1), 223–234. https://doi.org/10.1016/j.colsurfa.2004.10.114

Yaghmur, A., Aserin, A., & Garti, N. (2002). Furfural−cysteine model reaction in food grade nonionic oil/water microemulsions for selective flavor formation. *Journal of Agricultural and Food Chemistry, 50*(10), 2878–2883. https://doi.org/10.1021/jf011158l

Yeo, H., Balagiannis, D. P., Koek, J. H., & Parker, J. K. (2022). Comparison of odorants in beef and chicken broth — Focus on thiazoles and thiazolines. *Molecules, 27*(19), 6712. https://doi.org/10.3390/molecules27196712

Zamora, R., & Hidalgo, F. J. (2005). Coordinate contribution of lipid oxidation and Maillard reaction to the nonenzymatic food Browning. *Critical Reviews in Food Science and Nutrition, 45*(1), 49–59. https://doi.org/10.1080/10408690590900117